Enhancing clay adsorption properties: a comparison between chemical and combined chemical/thermal treatments

Youssef El Ouardi, Véronique Lenoble, Catherine Branger, Katri Laatikainen, Bernard Angeletti, Abdelkrim Ouammou

Enhancing clay adsorption properties: a comparison between chemical and combined chemical/thermal treatments.

Youssef El Ouardi[a-b-c], Véronique Lenoble[a*], Catherine Branger[b], Katri Laatikainen[d], Bernard Angeletti[e], Abdelkrim Ouammou[c]

[a]*Université de Toulon, Aix Marseille Univ, CNRS, IRD, MIO, France*

[b]*Université de Toulon, MAPIEM, Toulon, France*

[c]*Université Sidi Mohamed Ben Abdellah, Faculté des Sciences Dhar El Mehraz, LIMOM Laboratory, Dhar El Mehraz B.P. 1796 Atlas, Fès 30000, Morocco*

[d]*Lappeenranta-Lahti University of Technology, Laboratory of Computational and Process Engineering, P.O. Box 20, FI-53851 Lappeenranta, Finland*

[e]*Aix Marseille Univ, CNRS, IRD, INRA, Coll France, CEREGE, Aix-en-Provence, France*

* Corresponding author: lenoble@univ-tln.fr (V. Lenoble).

Abstract

A Moroccan bentonite was activated by sodium carbonate (Na-Be), and by a combined chemical and thermal activation (Na-Be450). The materials characterization was performed by XRD, EDS, FTIR, SEM and porosity measurements. The efficiency of Na-Be and Na-Be450 as low-cost adsorbents to remove nickel and silver from aqueous solution was checked. The Langmuir, Freundlich and Langmuir-Freundlich models were used for the analysis of equilibrium isotherms. Na-Be and Na-Be450 demonstrated a good removal efficiency towards nickel and silver, even in complex effluents (industrials wastewaters). The regeneration study proved that Na-Be450 presented all the characteristics of an efficient material for nickel removal.

Keywords: bentonite, chemical activation, thermal activation, adsorption, nickel, silver.

1. Introduction

The fight against environmental pollution has become the priority of many agencies/associations and commissions for environmental protection in the entire world. All pollutants from industrial or human origin can have very serious consequences for animals and plants (Qing et al., 2015; Yang et al., 2018). For example, discharges of polluted water from factories into rivers kill thousands of aquatic creatures like fishes (Islam and Tanaka, 2004; Mulk et al., 2016). In general, among the chemical substances likely to constitute a danger for aquatic life, metal elements like Ag, As, Cu, Cr, Ni, Pb, or Zn (Aithani et al., 2020; Lin et al., 2016) rank on top. These elements are increasingly used in many industrial sectors (Nagajyoti et al., 2010; Rivera et al., 2007). Consequently, there is a necessity to treat industrial effluents contaminated with metals before their discharge into the receiving water bodies. In Morocco, the craft sector is a buoyant and dynamic sector of the country's economy, especially developed in the region Fez-Meknes, where the brassware industry poses a significant risk for the environment by releasing effluents heavily contaminated by nickel and silver.

In recent years, nickel and silver in wastewater pose a very serious threat for ecosystems and human health (Dey et al., 2018; Mousavi et al., 2015). Nickel, a metal known to be carcinogenic, is widely used in modern industries (Dey et al., 2018). In addition, the exposures to small quantities of nickel on a long timescale can cause irritation and allergic reactions, in particular itchy skin (Das et al., 2008). Silver is considered as an emerging contaminant due to its increasing use based on its bactericidal properties (Fabrega et al., 2011; Maillard and Hartemann, 2013). Exposures to silver over a long period can lead to the appearance of a characteristic irreversible pigmentation of the skin and/or the eyes

(Gulbranson et al., 2000). The United States Environmental Protection Agency (US EPA) has set specific nickel limits for wastewater effluents: 0.2 mg/L for long-term effluent reuse and 2 mg/L for short-term effluent reuse.(Katsou et al., 2010) The US EPA, under the safe drinking water act, sets the contaminant level for silver in drinking water at 0.1 mg/L.(S. F. Etris, 2010) The European Directive 98/83/EC on the quality of water intended for human consumption sets a limit for nickel in drinking water at 20 µg/L.(EU, 1998) European Environmental Quality Standards (EQS) recommends that the silver concentration in drinking water does not exceed 5µg/L.(Vorkamp and Sanderson, 2016). Recently, there has been a considerable effort to develop efficient technologies to lower the levels of metal elements in water intended for human consumption. The conventional technologies for removing metals from wastewater include many processes such as precipitation (Fu and Wang, 2011), ion exchange (Da and Robens, 2004), adsorption (Dotto et al., 2015; El Ouardi et al., 2020), coagulation (El Samrani et al., 2008) and reverse osmosis (Bódalo-Santoyo et al., 2003). Among these, adsorption received considerable interest due many advantages over conventional methods (i.e., chemical precipitation, ion exchange, membrane filtration and coagulation-flocculation) such as the low cost, the high efficiency and the regeneration of the adsorbents.

The effectiveness of removing pollutants (such as metals) from effluents through an adsorption process strongly depends on the physical properties and chemical composition of the adsorbents (Uddin, 2017). Various natural adsorbents have been used in the adsorption process: kaolinite (Zhu et al., 2018), activated carbon (Zaini et al., 2010), natural and synthetic zeolites (Motsi et al., 2009) or clays (Uddin, 2017). The cost of the adsorbent is a key point for its commercial and industrial use. Recently, the use of bentonite for adsorption or removal of heavy metals in effluents has been the focus of

many studies because of its important economic benefits (Karapinar and Donat, 2009; Mohammed-Azizi et al., 2013; Vieira et al., 2010a). To increase the application range of bentonite use, there is a need to improve its physico-chemical properties. Numerous physical and chemical methods have been examined in that purpose, such as acid activation (España et al., 2019), heat treatment (Freitas et al., 2017) and treating with a cationic surfactants (Özcan et al., 2007). Nevertheless, none of the above-mentioned works did study the impact of such bentonite activation neither on nickel and silver retention nor on the competition of divalent metal ions such as nickel with monovalent metal ions silver for the adsorption sites.

The aim of this study was to activate bentonite with sodium carbonate (Na-Be) and by combined chemical and thermal activation (Na-Be450), to increase its adsorption capacity to remove nickel and silver from simple and complex media. The main purpose of the activation bentonite by sodium carbonate is the modification of its physico-chemical properties by modifying its specific surface area and increasing its cation exchange capacity. Furthermore, in this work, the chemical activated (Na-Be) will be subjected to thermal activation by heating at 450 °C (Na-Be450) to enhance its adsorption performance towards nickel and silver. The idea was to take advantage of the demonstrated improving effect of thermal treatment on materials (El Ouardi et al., 2020) and to compare with chemical activation, a simpler activation method. The materials were tested in a matrix of increasing complexity to finally be tested in natural effluents: tap water, river water as well as effluents from brassware industry. In view of a potential industrial process, the material regeneration was also checked.

2. Materials and Methods

2.1. Reagents and vessel

MilliQ water (resistivity 18.2 MΩ, TOC < 10 µg/L, Millipore, Milli-Q system) was used to prepare all the solutions mentioned below. Nickel (II) nitrate hexahydrate ($Ni(NO_3)_2.6H_2O$, 99.9%) was used as received from Sigma Aldrich. Ag (I) Silver nitrate ($AgNO_3$, ≥99.7%), sodium carbonate (Na_2CO_3, ≥99.5%) were used as received from Fisher Scientific. N-(2-Hydroxyethyl)piperazine-N-2-ethanesulfonic Acid (HEPES, ≥99 %) from Fisher Scientific was used to buffer the solutions.

For all experiments, vessels (Corning® tubes, syringes, filters, etc.) were pre-cleaned before use with HNO_3 washing (10%, Fisher, Analytical Grade) then thoroughly rinsed with milliQ water.

2.2. Solids preparation

In this study, a natural bentonite was sampled in Trebia deposit in northeastern Morocco. The raw bentonite was sieved and the fraction below 100 µm was collected. Then, the material was firstly activated by chemical activation with 4% (w/w) of sodium carbonate (4 g sodium carbonate/100 g bentonite). Na_2CO_3 was added to a suspension of bentonite in boiling water (about 500 mL, MilliQ water). The mixture was boiled for 1 hour and then the dispersion was cooled and allowed to settle. The supernatant was filtered, and the settled bentonite was washed twice with deionized water. Finally, the solid was collected and dried in an oven at 105 °C (Yildiz et al., 1999). A sample of the chemically-modified bentonite (Na-Be) was then submitted to heating treatment under air at 450°C, in a programmable furnace applying a heating rate of 5 °C/min, with a constant cooling rate of 5 °C/min. The samples of were left in the furnace for 24h at the calcination temperature. The obtained materials will hereafter be labelled as Raw-Be for raw

bentonite, Na-Be for the modified bentonite by chemical activation, then Na-Be450 for the modified bentonite by combined chemical and thermal activation.

2.3. Solids characterization

Powder X-ray diffraction (XRD) patterns of the samples were obtained with a X'Pert Pro panalytical diffractometer using a CuK_α radiation at 40 kV and 30 mA with a scan range of 5–70 °2θ, a scan speed of 0.02 °2θ per 2s, and a step size of 0.02 °2θ.

Fourier-Transform InfraRed (FTIR) spectra were obtained on a Bruker Vertex70 spectrometer equipped with a D-LaTGS-detector (L-alanine doped triglycine sulfate). About 1 mg of sample was mixed with approximately 300 mg of dried KBr and pressed to get pellets. The measurements were carried out over the range 4000–400 cm^{-1} in the transmittance mode, with a spectral resolution of 4 cm^{-1}.

For scanning electron microscopy (SEM) and energy dispersive X-ray spectroscopy (EDS), samples were metalized by a thin gold layer and SEM images were taken using a Supra 40 VP microscope (Gemini). This equipment has an Oxford 7060 X-ray spectroscopy system through dispersive energy (EDS), which enables qualitative evaluation of the chemical composition.

The specific surface areas were determined according to the Brunauer Emmet–Teller (BET) equation with nitrogen adsorption–desorption isotherms at 77K using a Micrometrics Gemini V apparatus.

2.4. Adsorption experiments

Aqueous solutions of nickel and silver were prepared by dissolving $Ni(NO_3)_2 \cdot 6H_2O$ and/or $AgNO_3$, in milliQ water to reach the desired concentrations. For all experiments, trace metal concentrations in solution were measured using ICP-OES (Perkin Elmer - Optima 7300 DV).

The kinetic studies determination was carried out at room temperature and pH 7.0 (using HEPES buffer) in 50 mL Corning© tubes by mixing 0.4 g of adsorbent to 40 mL of a 50 mg/L nickel solution. The samples were shaken for a time interval between 0 and 72h.

The batch adsorption experiments were carried out at room temperature in 50 mL Corning© tubes by mixing a fixed amount of adsorbent (0.4 g) with 40 mL of aqueous solution of nickel or silver. The mixture was shaken with an orbital shaker at a speed of 80 rpm during 90 min. The pH of the dispersions was adjusted to 7.0 using HEPES buffer. All experiments were carried out in duplicate. At the end of adsorption experiments, dispersions were centrifuged at 5000 rpm for 5 min. The supernatant was then filtered with syringe filters (0.45µm, Surfactant - Free Cellulose Acetate, Sartorius). The filtrates were acidified with suprapur® HNO_3 at pH < 2 and stored at 4 °C before analysis for their nickel and silver content.

Equilibrium isotherms for nickel and silver were obtained by performing batch adsorption studies: nickel and silver retention were studied on Raw-Be, Na-Be and Na-Be450 over a wide concentration range, from 15 to 120 mg/L. These values were chosen to frame the real contaminant levels in the most contaminated considered effluent (around 80 and 42 mg/L for nickel and silver, respectively, Table 1).

As Na-Be and Na-Be450 gave the most promising results, they were further used for the simultaneous removal of nickel and silver for the rest of the experiments.

Nickel and silver competition on Na-Be and Na-Be450 were studied in binary-component system. The experiments were carried out a mass ratio of 1:1 Ni:Ag, with nickel and silver concentrations equally ranging between 15 to 120 mg/L in buffered milliQ water at pH 7 for 90 min.

Nickel and silver retention on Na-Be and Na-Be450 were studied in real effluents by batch adsorption experiments. Effluents from the brassware industry (A) and effluents from Sebou (S1, S2) and Fez (F1, F2) rivers were tested in this study. Effluent brassware was directly collected into the rinsing baths before discharge in Fez river. The effluents from Fez and Sebou rivers were collected downstream from Fez city and downstream from the confluence with Fez river respectively, either during a period of brassware fabrication (F1 and S1) or during a non-working day (F2 and S2). The composition of each effluent is presented in Table 1 and Table SI-1.

Table 1. Physico-chemical characterization of the tested effluents: brassware (A), and Fez (F1 and F2) and Sebou (S1 and S2) rivers. Index 1 refers to a period of brassware fabrication and index 2 refers to a non-working day.

	Ni (µg/L)	**RSD %**	**Ag (µg/L)**	**RSD %**	**pH**
A	$80.3 \cdot 10^3$	1.3	$41.7 \cdot 10^3$	0.31	8.55
F1	214.6	7.2	94.3	1.8	7.12
F2	59.5	1.4	51.1	1	6.67
S1	122.8	1.4	28.9	2.4	7.11
S2	20.4	2.6	5.1	1.1	6.96
EQS	20	-	5	-	-

EQS: Environmental Quality Standard.
RSD: Relative Standard Deviation.

In order to examine the reusability of the adsorbent, the used material was agitated with 10 mL of 0.05 mol/L HNO_3 for 30 min, the procedure was repeated as long as trace metals could not be detected. They were then washed three times with milliQ water to remove acidity. Finally, the adsorbent was dried at 60 °C for 24h. Then, nickel and silver

adsorptions were repeated in the same conditions as before. The regeneration cycle was repeated five times.

2.5. Theoretical and calculations fundamentals

Several kinetic models can be used to express the adsorption mechanism of solute on an adsorbent. The amount of the metal ion adsorbed per unit mass of the adsorbent at equilibrium, q_e (mg/g), and the adsorption rate (%) were calculated from the expressions:

$$q_e = \frac{(C_0 - C_e)}{m} . V \qquad (1)$$

$$\% \text{ Adsorption} = \frac{(C_0 - C_e)}{C_0} .100 \qquad (2)$$

where C_0 (mg/L) is the metal ion initial concentration in the solution, Ce (mg/L) is the metal ion concentration at equilibrium in the dissolved phase, m is the mass of adsorbent (g) and V is the volume of solution (L).

In this work, the pseudo-first-order kinetic and the pseudo-second-order kinetic were used to study the kinetic behavior of nickel on the surface of the modified bentonite by chemical activation (Na-Be) and the modified bentonite by combined chemical and thermal activation (Na-Be450).

The kinetic model of pseudo-first-order proposed by Lagergren (Lagergren, 1898) is generally applicable over the initial 20 to 30 minutes of the adsorption process (Aksu, 2001). This model assumed that the adsorption process is reversible (Guimarães and Leão, 2014).

This model is expressed by the following equation:

$$q_t = q_e(1 - e^{-k1t}) \qquad (3)$$

Contrarily to the pseudo-first-order model, the pseudo-second-order kinetic model, developed by Ho and McKay (Mckay, 1998), predicts the behavior over the whole range

of adsorption time scale. The pseudo-second-order model is based on the assumption that the rate-limiting step may be chemisorption, which involves valence forces by electron sharing or exchange between the adsorbate and the adsorbent (Ho, 2006). The pseudo-second-order equation is given by the following expression:

$$Q_t = \frac{k_2 Q_e^{\,2} t}{1 + k_2 Q_e t} \qquad (4)$$

where k_1 is the rate constant of pseudo-first-order in min^{-1} and k_2 is the rate constant of pseudo-second-order in (g mg^{-1} min^{-1}) and q_t and q_e are the amount of solute adsorbed at time t and at equilibrium, respectively.

Equilibrium isotherms for nickel and silver were studied in order to better model the adsorption mechanisms.

The adsorption data were analyzed using Langmuir (Langmuir, 1918) and Freundlich (Freundlich, 1906) models. Langmuir model is based on a homogeneous surface with a finite number of identical sites. It also assumes that there is no interaction between the adjacent sites. Langmuir equation is expressed as:

$$q_e = \frac{q_m k_L C_e}{1 + k_L C_e} \qquad (5)$$

where q_m (mg/g) refers to the maximum adsorption capacity and K_L (L/mg) is the Langmuir constant.

Freundlich model supposes that adsorption occurs onto a heterogeneous surface. This model is expressed by the following equation:

$$q_e = K_F C_e^{1/n} \qquad (6)$$

where K_F and n are Freundlich constants related to the adsorption capacity and the strength of adsorption respectively.

The Langmuir–Freundlich equation (Sips, 1948) is given by:

$$q_e = \frac{q_m (K_{LF} C_e)^{n_{LF}}}{1+(K_{LF} C_e)^{n_{LF}}} \qquad (7)$$

where q_e is the adsorbed amount at equilibrium (mg/g), q_m the L–F maximum adsorption capacity (mg/g), C_e the adsorbate equilibrium concentration (mg/L), K_{LF} the equilibrium constant for a heterogeneous solid, and n_{LF} is the heterogeneity parameter.

Another parameter was considered: the rate of equilibrium adsorption reduction (Δ) (Zhi-rong and Shao-qi, 2009). It is the ratio of the difference between non-competitive equilibrium adsorption and competitive equilibrium adsorption to non-competitive adsorption observed at equilibrium:

$$(\Delta)\% = \frac{(q_i m - q_i mix)}{q_i m} \qquad (8)$$

where $q_i m$ (mg/g) and $q_i mix$ (mg/g) are the maximum adsorption capacity of i species in the single component system and binary component system, respectively.

To prove the fit quality, Pearson's chi-square (χ^2) values were evaluated using the the following equation (Piccin et al., 2017):

$$\chi^2 = \sum_{i=1}^{n} \frac{(q_{i,exp} - q_{i,model})^2}{q_{i,model}} \qquad (9)$$

Where $q_{i,exp}$ is the experimental value (mg/g) of an independent variable, $q_{i,mod}$ is the equilibrium capacity calculated with the model (mg/g), n is the number total of information.

3. Results and discussion

3.1. Physico-chemical characterization of the considered materials

Fig.1 presents the XRD patterns of the raw bentonite (Raw-Be) and modified bentonites by chemical activation (Na-Be) and combined chemical and thermal activation (Na-

Be450). The phases were identified using X'Pert Highscore software through the JCPDS database. The studied bentonites mostly consist of montmorillonite (Mt), feldspars (F) and small amounts of crystalline phases in the form of impurities quartz (Q). For Raw-Be, all peaks were located at 2θ = 5.9° (d= 14.9 Å), 19.8° (d= 4.4 Å), 34.1° (d= 2.6 Å), 35.8° (d= 2.5 Å) and 62.2° (d= 1.49 Å). Values of d-spacing = 14.9 Å, 4.4 Å, 2.6 Å, 2.5 Å and 1.49 Å, which correspond to the montmorillonite according to JCPDS database. Feldspars peak (F) [2θ = 27.7°] and quartz peak (Q) [2θ = 26.6°] with values of d-spacing = 3.2 Å and 3.3 Å for Feldspars and Quartz respectively, could also be observed. The estimation of montmorillonite and feldspars in the materials were evaluated by Diffrac.eva using semi quantitative method and led to the following proportions: 70.0 to 73.4% of Montmorillonite, 25.6 to 27.0% of Feldspars and 1 to 3 % of other phases. D-spacing series of smectites for Raw-Be demonstrated a reflection (d_{001}) at d-value of 14.9 Å. This diffraction peak shrinked to 13.3 Å after activation treatments. Thus, through the evolution of bentonite after activation treatments, a structural change can be noticed, especially the move of the characteristic montmorillonite peak at Bragg angles 2θ = 6.8°, which indicated a variation in sodium and calcium proportions (Table 2) as already demonstrated (El Miz et al., 2017). It has also to be noted the disappearance of the crystalline phases in forms of Quartz impurities (Q) with the activation treatments.

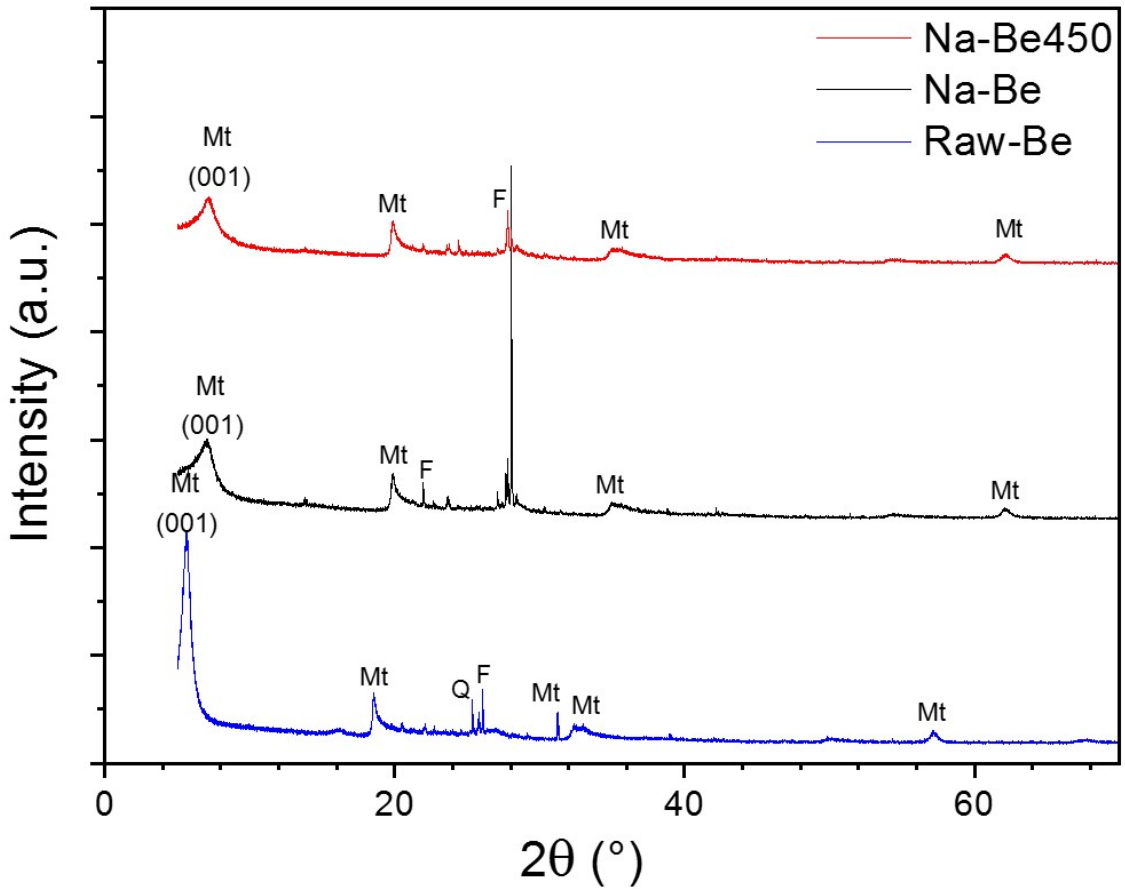

Fig.1. Powder XRD profiles of Raw-Be, Na-Be and Na-Be450. (Mt: Montmorillonite, F: Feldspar, Q: Quartz).

Table 2. Chemical composition of bentonite analyzed by EDS

	Wt(%)		
	raw-Be	**Na-Be**	**Na-Be450**
Na	2.2±0.1	3.5±0.3	2.9±0.1
Mg	3.3±0.02	2.3±0.1	2.1±0.04
Al	24.1±0.02	24.6±0.2	25.3±0.12
Si	60.7±0.1	57.2±0.1	58.5±0.2
K	0.8+0.16	0.9±0.15	1.3±0.2
Ca	2.3±0.1	0.8±0.02	0.5±0.1
Fe	6.3±0.4	3.9±0.2	4.7±0.15

FTIR spectra of the natural and modified bentonite (Fig.2) showed infra-red bands observed around 517 cm^{-1} corresponding to the deformation modes of Si-O-Al (Er-ramly, 2014), while the bands at 910 and 840 cm^{-1} are the characteristic bands of the bending vibrations of the Al-Mg-OH and Al-Al-OH groups of bentonite (Ayari et al., 2005; Bertagnolli et al., 2011; Farmer, 1974; Xu et al., 2000). The presence of adsorbed water is evidenced by the band at 1635 cm^{-1}, characteristic of the bending vibration of H_2O. The strong band at 1000 cm^{-1} of raw-Be can be attributed to a Si-O stretching vibration of the condensed phase, affected by Si-O-H deformation vibration band (G. Socrates, 2001), while the band at 3396 cm^{-1} corresponds to water stretching vibration band, and 3623 cm^{-1} to the stretching vibration of structural OH groups (Farmer, 1974).

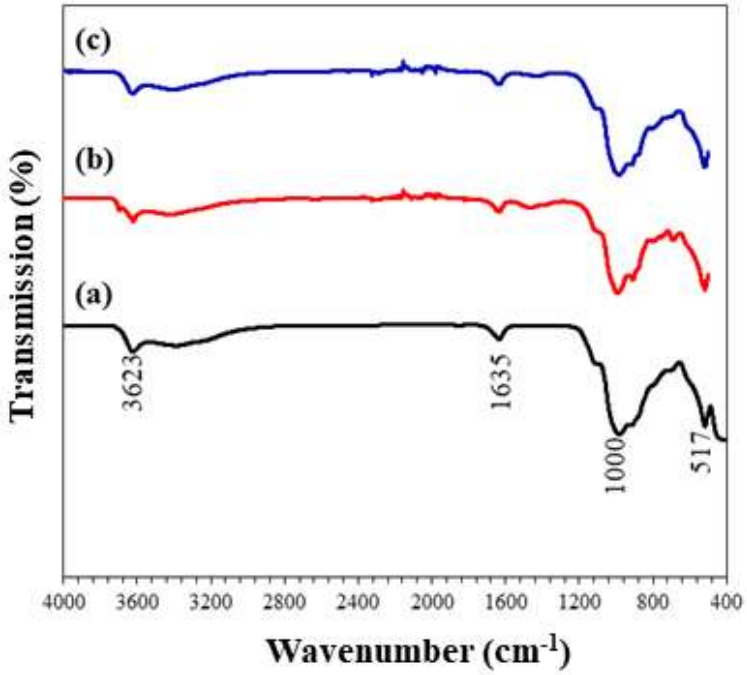

Fig.2. FTIR spectra of raw-Be (a), Na-Be (b) and Na-Be450 (c).

3.2. Morphology and characterization of the considered materials

The morphology of Raw-Be (Fig. 3a), Na-Be (Fig. 3b) and Na-Be450 (Fig. 3c) showed an irregularity of the particles forming aggregates. The SEM pictures showed the classical general appearance of the montmorillonite, essentially constituted of sheets. As a matter of fact, smectites are demonstrated to be composed of one octahedral sheet centered between two tetrahedral sheets (Shichi and Takagi, 2000; Uddin, 2017). As seen from Figs. 3b to 3c, the evolution of modified bentonite grain size during activation process could be observed. Fig. 3b and 3c showed a slight increase in particle roughness resulted by activation treatment.

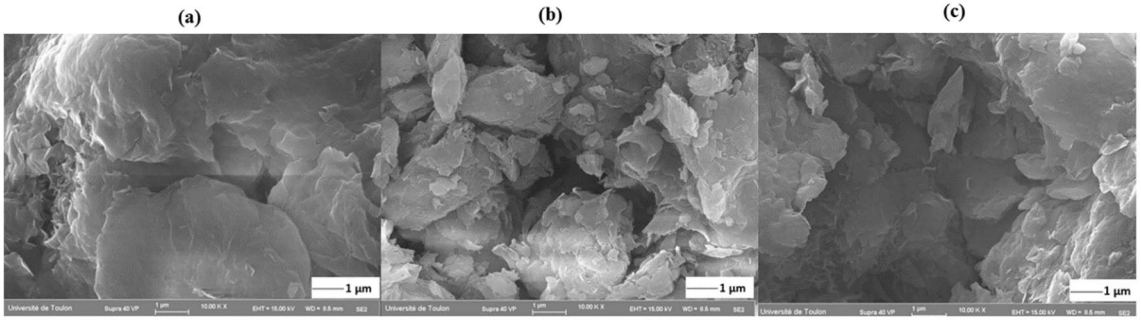

Fig.3. SEM images of Raw-Be (a), Na-Be (b) and Na-Be450 (c).

Table 3. Surface area, total pore volume, and pore diameter of raw bentonite and modified bentonites.

Materials	BET surface area (m^2/g)	Total pore volume (cm^3/g)	Average pore diameter (nm)
Raw-Be	14.5	0.063	4.9
Na-Be	44.9	0.078	6.6
Na-Be450	66.7	0.1	6.7

Nitrogen adsorption/desorption experiments were performed on Raw-Be, Na-Be and Na-Be450 to study their porosity. Fig. 4a shows that the isotherms of modified bentonites are of type IV according to the IUPAC classification (Stafford et al., 1985; Thommes et al., 2015), which reveals the presence of mesopores in these materials. The specific surface area (determined by BET) and total pore volume of raw bentonite were 14.5 m^2/g and

0.063 cm^3/g, respectively. When considering Na-Be and Na-Be450, an increase in the BET surface area (44.9. m^2/g and 66.7 m^2/g respectively, Table 3) was measured. Na-Be450 bentonite has received maximum improvement in surface area (78%), compared to Na-Be (67%). The pore size of the modified bentonites followed the same trend as the specific surface area: Na-Be450 > Na-Be > Raw-Be. Na-Be and Na-Be450 were composed of micropores, mesopores and macropores (Fig. 4b). It can be concluded that the treatment has resulted in an important increase in specific surface and pore size, with a higher effect of the combined treatment. This is due to the removal of adsorbed and hydrated water molecules, and other impurities.

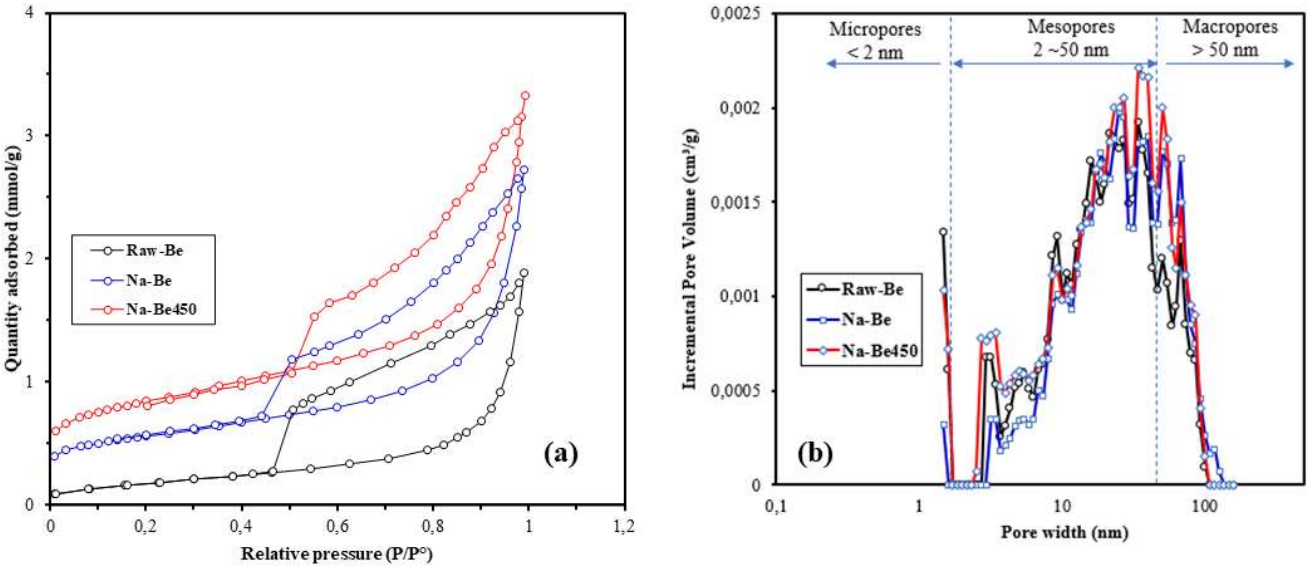

Fig.4. Nitrogen adsorption-desorption isotherms (a) and pore size distributions (b) for modified bentonites Raw-Be, Na-Be and Na-Be450.

3.3. Kinetic studies of nickel retention

The kinetic studies of nickel onto modified bentonites are presented in Fig. 5. The adsorption of nickel ions on modified bentonite was demonstrated to rapidly occur. The maximum adsorbed amount of nickel on Na-Be and Na-Be450 were 4.6 and 4.8 mg/g, respectively (Fig. 5). The adsorption kinetics of nickel on Na-Be and Na-Be450 are examined with the pseudo-first-order and the pseudo-second-order kinetics (Fig. 5). Table

4 shows the different kinetic parameters calculated from the graphical representation of these three models. According to the coefficient of determination (R^2) values and the q_{eq} values (Table 4), the pseudo-second-order kinetic model is the most reliable to describe the adsorption of nickel on the modified bentonites, which suggests that the adsorption process may be a chemisorption (Kumar et al., 2011; Piccin et al., 2017; Zou et al., 2006).

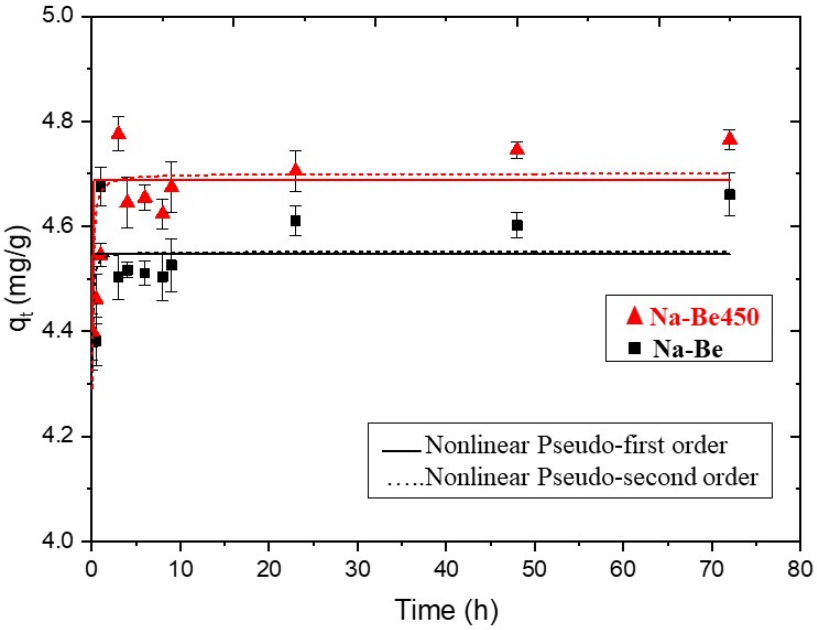

Fig.5. Kinetic curve for nickel adsorption on Na-Be and Na-Be450. Solid lines and dash-dotted represent pseudo-first-order kinetic model fitting, and pseudo-second-order kinetic model, respectively.

Table 4. Ni(II) adsorption rate coefficients for pseudo-first-order and pseudo-second-order models on Na-Be and Na-Be450.

Model	Parameter	Adsorbent	
Pseudo first order		Na-Be	Na-Be450
	q,exp (mg/g)	4.6	4.8
	$q_{,cal}$ (mg/g)	4.54	4.68
	K_1 (1/h)	0.66	0.56
	$\chi 2$	5.71	12.47
	R^2	0.98	0.96
Pseudo second order	$q_{,cal}$ (mg/g)	4.55	4.7
	K_2 (mg/g.h)	0.99	0.21
	$\chi 2$	5.38	9.38

	R^2	0.99	0.99

3.4. Nickel and silver retention in single-component systems

The equilibrium isotherms in single component systems are presented in Fig.6. The maximum nickel retention capacity (10.7 mg/g) was obtained for the modified bentonite by combined chemical and thermal activation (Na-Be450). The obtained results fully followed the variation of specific surface with activation treatment S_{BET} (Na-Be450) > S_{BET} (Na-Be)) > S_{BET} (Raw-Be). In addition, nickel adsorption on Raw-Be in the tested experimental conditions caused the saturation of the adsorption sites of the considered material, compared to the activated bentonite which still demonstrated adsorption properties. This means that the activated treatment of Na-Be and Na-Be450 creates more active sites, leading to an improved retention ability.

The adsorption capacity for silver more rapidly reached saturation than for nickel, on each of the tested material. The maximum silver retention capacity (7.1 mg/g) was obtained for the modified bentonite by combined chemical and thermal activation (Na-Be450), which corroborates the results obtained for nickel.

Adsorption isotherms were modeled by Langmuir (Eq (5)), Freundlich (Eq (6)), and L-F models (Sips) (Eq (7)). Based on the coefficient of determination (R^2) values (Table 5), Freundlich does not provide a good fit to the experimental data for both nickel and silver ions. The experimental data have been well fitted by Langmuir isotherm and Langmuir-Freundlich (Sips) models as can be observed in Table 5 and Fig.6. These results predict

a cooperative adsorption process involving adsorbent-adsorption interactions, which implies that the adsorbents present homogeneous adsorption sites (Guerra et al., 2013). The adsorption of nickel and silver ions may also be enhanced by ion exchange which occurs between the metal ions and the amounts of alkali and alkaline-earth metals in bentonites (e.g. Ni^{2+} can take the place of the exchangeable cations such as Na^{+}, Mg^{2+} and K^{+} in bentonite layer and interposed between the bentonite layers) (Vieira et al., 2010a). As a matter of fact, the exchange process between sodium and calcium occurring during chemical treatment and demonstrated by EDS and XRD analysis, could enhance the adsorption capacities, as already demonstrated (Alvarez-Ayuso and Garcia-Sanchez, 2003; Bhattacharyya and Gupta, 2008; Ijagbemi et al., 2010). The results from this study suggests that the chemical activation (Na-Be) and the combined chemical and thermal activation (Na-Be450) could be an effective method to enhance the adsorption capacity of the bentonite.

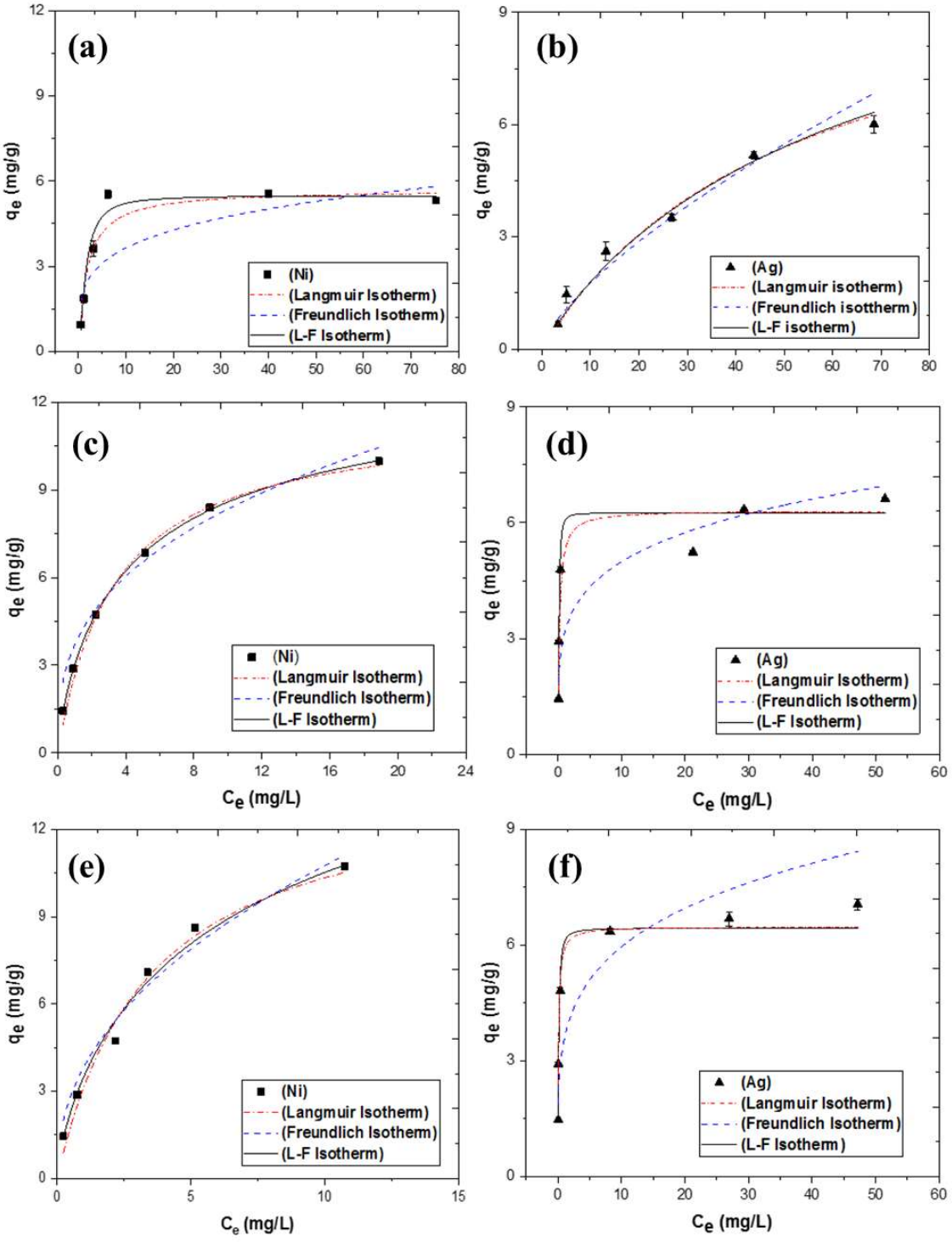

Fig.6. Equilibrium isotherms for Ni adsorption onto (**a**) Raw-Be (**c**) Na-Be and (**e**) Na-Be450 as well as equilibrium isotherms for Ag adsorption onto (**b**) Raw-Be (**d**) Na-Be and (**f**) Na-Be450. Dotted, dash-dotted and solid lines represent Langmuir fitting, Freundlich and Langmuir-Freundlich fitting, respectively.

Table 5. Langmuir, Freundlich and L-F parameters for Ni and Ag retention onto Raw-Be, Na-Be and Na-Be450 in single component systems.

System	Metal	Model	Parameter	Adsorbent		
Single-component system	Ni	Langmuir		Raw-Be	Na-Be	Na-Be450
			$q_{,exp}$ (mg/g)	5.6	9.9	10.7
			q_m (mg/g)	5.5	11.6	13.9
			K_L	0.75	0.3	0.29
			$\chi 2$	5.3	0.18	0.14
			R^2	0.998	0.995	0.994
		Freundlich	1/n	0.32	0.35	0.45
			K_F	1.82	3.7	3.8
			$\chi 2$	3.4	1.28	6.5
			R^2	0.755	0.959	0.974
		L-F	q_m (mg/g)	5.5	13.8	19.6
			K_{LF}	0.52	0.29	0. 12
			n_{LF}	0.94	0.78	0.72
			$\chi 2$	2.2	0.018	0.034
			R^2	0.98	0.999	0.997
	Ag	Langmuir	$q_{,exp}$ (mg/g)	6	6.6	7.1
			q_m (mg/g)	9.1	6.3	6.5
			K_L	0.028	4.6	9.5
			$\chi 2$	6.5	2.5	0.035
			R^2	0.946	0.968	0.958
		Freundlich	1/n	0.67	0.2	0.22
			K_F	0.38	3.13	3.54
			$\chi 2$	2.1	4.3	3.3
			R^2	0.95	0.943	0.784
		L-F	q_m (mg/g)	12.5	6.25	6.4
			K_{LF}	0.02	6.5	7.1
			n_{LF}	1.5	1.7	1.4
			$\chi 2$	0.87	2.4	5.3
			R^2	0.99	0.976	0.974

3.5. Nickel and silver retention in binary-component systems

When simultaneously exposed to nickel and silver, the maximal adsorption capacities obtained for Na-Be450 equaled 10.2 and 6.6 mg/g (or 0.17 and 0.06 mmol/g) for nickel and silver, respectively (Fig.7). This is in agreement with the above results in single component systems. The results obtained in single component systems were added on the figures for an easier comparison, showing that the competition led to a decrease of the adsorption capacity, but such reduction was attenuated for the modified bentonites.

Following the previous modelling results, only L-F model was used (Table 6) to fit the experimental data in binary-system. The high R^2 values showed that equilibrium data were well-fitted, which corroborates the previous results in single component system suggesting a monolayer adsorption of nickel and silver onto Na-Be and Na-Be450.

In terms of competition between metals, such enhanced competitive effects in binary-components was investigated (Mohan and Singh, 2002; Zhi-rong and Shao-qi, 2009) using the ratio of the maximum adsorption capacity for the metal in the binary-component system (q_{imix}) to the maximum adsorption capacity for the same metal in the single-component (q_{im}). If $q_{imix}/q_{im} > 1$, the adsorption is promoted in the presence of the other metal ions); if $q_{imix}/q_{im} = 1$, there is no effect and interaction between metal ion i and other metals ions; if $q_{imix}/q_{im} < 1$, the adsorption is suppressed by the presence of other metal ions. In this work, the values of all q_{imix}/q_{im} were below 1, which confirms the mutual competitive effect of nickel and silver in binary component systems. The rates of equilibrium adsorption reduction (Δ) are given in Table 6. For Na-Be, the rate of equilibrium adsorption reduction (Δ) of nickel was diminished by 6.4% in binary-component system (Ni-Ag), and for silver was decreased by 25.6% in the (Ag-Ni) system. For Na-Be450 in Ni(Ni-Ag) and Ag(Ag-Ni) systems, this rate (Δ) was decreased by 4.6%

and 5.8%, respectively. These results were in agreement with the observed experimental data (Fig. 7). Based on the rate of equilibrium adsorption reduction (Δ) values, the modified bentonite by combined chemical and thermal activation (Na-Be450) has demonstrated its performance and efficiency towards nickel and silver even in the binary component system. In addition, it was clear that the presence of another metal led to a competition for the adsorption sites on Na-Be and Na-Be450, even though nickel was less submitted to this effect compared to Ag. This could be explained by the smaller ionic radius of nickel (0.72 Å) (Yavuz et al., 2003) than that of silver (1.26 Å) (Liu et al., 2003) which allows an easier nickel penetration to the available sites of Na-Be and Na-Be450.

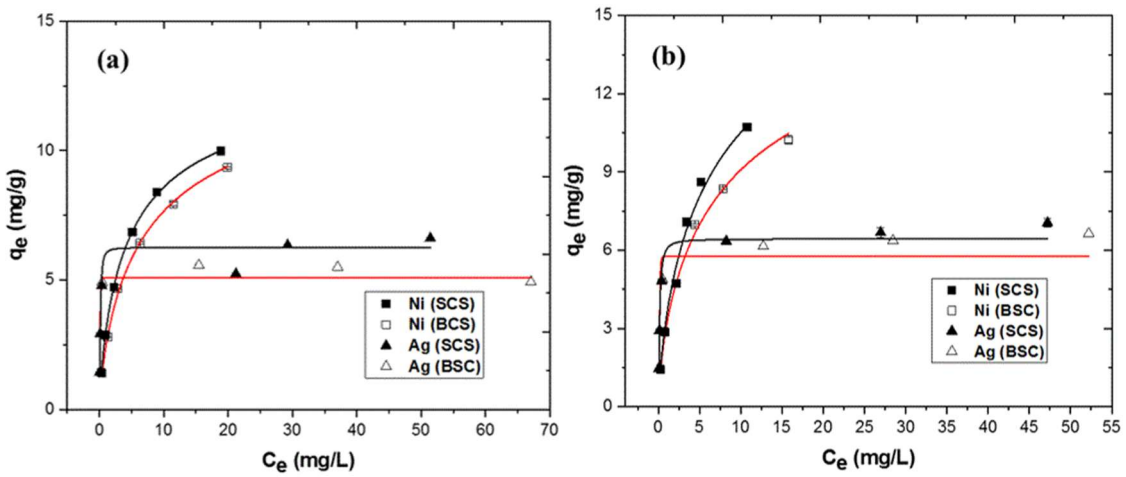

Fig.7. Equilibrium isotherms for **(a)** Ni adsorption onto Na-Be and Na-Be450 as well as equilibrium isotherms for **(b)** Ag adsorption onto Na-Be and Na-Be450. Solid lines represent Langmuir-Freundlich fitting. (SCS: Single Component System, BCS: Binary Component System).

Table 6. L-F parameters for Ni and Ag retention onto Na-Be and Na-Be450 in binary component systems.

System	Metal	Model	Parameter	Adsorbent	
Binary component systems	Ni(Ni-Ag)	L-F		Na-Be	Na-Be450
			q_{exp} (mg/g)	9.3	10.2
			q_m (mg/g)	13.4	18.1
			K_{LF}	0.2	0.1
			n_{LF}	0.76	0.67

	χ^2	1.3	1.1
	R^2	0.999	0.997
	Δ (%)	6.4	4.6
Ag(Ag-Ni)	q_{exp} (mg/g)	4.9	6.6
	q_m (mg/g)	5.1	5.7
	K_{LF}	1.2	2.5
	n_{LF}	3.1	3.8
	χ^2	1.7	2.1
	R^2	0.985	0.972
	Δ (%)	25.6	5.8

3.6. Nickel and silver retention in natural effluents.

To better understand the mechanism of silver adsorption by bentonites in complex environments, it is important to know the speciation of silver in solution which also depends on the pH. Speciation diagram of silver was obtained using the Hydra-Medusa software Figure SI.1. The choice of the concentrations studied in the Figure SI.1 was based on the values found in the natural effluents such as brassware effluent (A), Fez (F1) and Sebou rivers (Table 1) and tap water (Table SI.2).

Nickel and silver retention by Na-Be and Na-Be450 in tap water are depicted in Fig.8. The results obtained with milliQ water (MQ) experiments were added on the figures for an easier comparison. The presence of some major ions (i.e., calcium, sodium and magnesium, … Table SI-2) in tap water did not seem to impact on modified bentonites efficiency. Silver retention quite increased compared to that in milliQ water experiments. This result could come from the presence of chloride ions in tap water (37 mg/L) that could directly increase silver removal accounted for Na-Be and Na-Be450 material. The probability of formation of silver chloride solid was performed using the Hydra-Medusa software (Ignasi Puigdomenech, 2015). As a function of Cl/Ag ratios, the results of the

Hydra-Medusa simulation (Fig. SI-1) confirmed the formation of AgCl(s). Concerning nickel, the results showed that the removal efficiency in the studied concentration range were above 89% and 93% on Na-Be and Na-Be450, respectively. Silver removal efficiency on Na-Be and Na-Be450 was above 99 %. In these conditions, the modified bentonites have demonstrated a good adsorption efficiency, which turns these adsorbents interesting for metal adsorption, even in complex media.

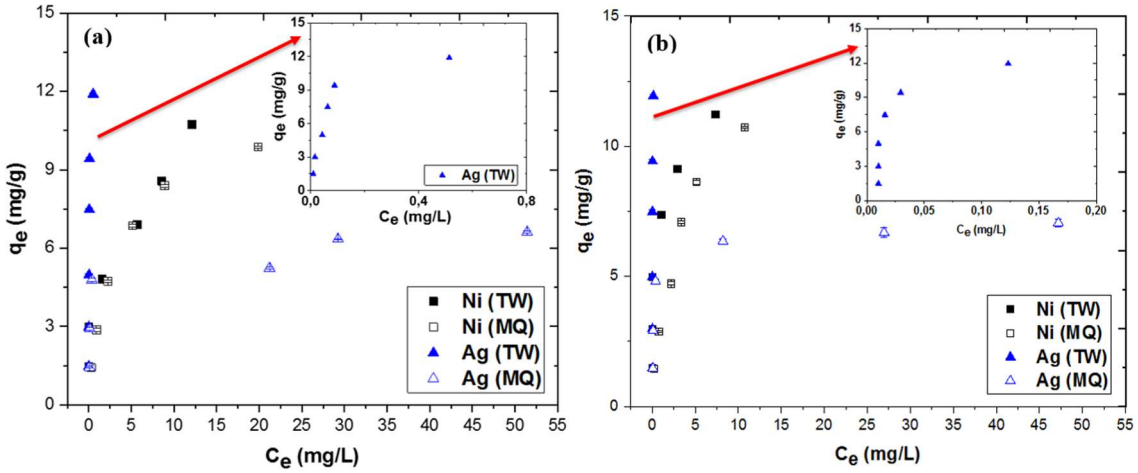

Fig.8. Adsorption of nickel and silver adsorption onto Na-Be and Na-Be450 in tap water (TW). The results obtained in milliQ water (MQ) are presented for an easier comparison.

The brassware effluent (A) was characterized by very high metal levels: 80.3 mg/L of nickel and 41.7 mg/L of silver (Table 1). The effluents from Fez (F1) and Sebou rivers (S1) during working day were polluted in nickel and silver, though at a lesser extent: 214.6 and 94.3 µg/L, respectively, in Fez river and 122.8 and 28.9 µg/L, respectively, in Sebou river. Fez (F2) and Sebou rivers (S2) during non-working day were the least polluted in nickel and silver: 59.5 and 51.1 µg/L, respectively, in Fez river and 20.4 and 5.1 µg/L, respectively, in Sebou river (Table 1).

In order to assess the risk associated with the presence of metal pollutants in the studied waters, the measured concentrations were compared to the standards set by the European Water Framework Directive (Directive, 2008/105/EC). The results showed that nickel

and silver concentrations in the study sites are greater than the values set for nickel (20 µg/L) (EU, 2008) and silver (5 µg/L) concentrations (Vorkamp and Sanderson, 2016), established in accordance with Environmental Quality Standards (EQS). This means that the waters of Fez and Sebou rivers present a toxic risk for aquatic organisms.

The retention of nickel from the brassware industry effluent (A) by Na-Be and Na-Be450 turned less efficient due to the presence of numerous competing agents. Na-Be and Na-Be450 retention efficiency were 26.4 and 41.2% respectively for Ni. Such discrepancy can be explained by the higher surface area of the modified bentonite by combined chemical and thermal activation (Na-Be450), which caused an increase of the number of available sites. Silver removal efficiency is very high. This result may be due to the presence of ions (chloride for example) in effluents wastewater which could react with silver and lead to precipitation.

The removal efficiency of Na-Be and Na-Be450 for both nickel and silver in Sebou and Fez rivers were 100% (Table 7). It has to be underlined that even if the tested effluents were less contaminated in metals than the brassware rinsing bath, their metals content was important. This clearly demonstrated the effectiveness and ability of both materials for removal nickel and silver in a complex and contaminated media.

Table 7. Removal efficiency towards nickel and silver from tested effluents: brassware (A), and Fez (F1 and F2) and Sebou (S1 and S2) rivers. Index 1 refers to a period of brassware fabrication and index 2 refers to a non-working day.

	Removal efficiency Ni %		**Removal efficiency Ag %**	
	Na-Be	Na-Be450	Na-Be	Na-Be450
A	26.4	41.2	100	100
F1	100	100	100	100

F2	100	100	100	100
S1	100	100	100	100
S2	100	100	100	100

In order to evaluate the potential improvements to nickel and silver ions extraction offered by modified bentonite by chemical activation (Na-Be) and the modified bentonite by combined chemical and thermal activation (Na-Be450) over other adsorbents, the results obtained in this work were compared to the retention capacities of some usual natural adsorbents from the literature (Table 8), chosen for their composition close to that of the studied bentonites. Although a direct comparison of Na-Be and Na-Be450 with other adsorbents is quite complicated due to the different experimental conditions used, it has been found that nickel and silver adsorption capacity of Na-Be and Na-Be450 is among the highest results. Therefore, considering the adsorption capacities of other natural materials, low cost, accessibility and environment friendly bio-material, it can be concluded that the modified bentonite by chemical activation (Na-Be) and the modified bentonite by combined chemical and thermal activation (Na-Be450) proved themselves promising low cost-effective natural adsorbents to remove nickel and silver ions from aqueous solutions.

Table 8. Comparison of nickel and silver adsorption capacity of natural adsorbents with composition close to that of the studied bentonite.

Metal	**Adsorbent**	**Particle size**	**pH**	**C_0 (mg/L)**	**q_{max} (mg/g)**	**References**
Ni	Modified montmorillonite (A-MMT)	-	2.3-9.8	50-100	7.78	(Ijagbemi et al., 2010)
	Un-calcined sodium exchanged (NaMMT)	-	2.3-9.8	50-100	9.93	(Ijagbemi et al., 2010)

	Alkaline-modified montmorillonite clay	100 µm	2-8	100-500	125.95	(Akpomie and Dawodu, 2014)
	Bofe bentonite	-	5.3	3-200	1.91	(Vieira et al., 2010b)
	Ca-bentonite	<100 µm	4	10-150	6.3	(Alvarez-Ayuso and Garcia-Sanchez, 2003)
	K10 montmorillonite clay	-	1-6	10-2000	2.1	(Carvalho et al., 2008)
	Sepiolite	-	7	0.01-1	2.24	(Ansanay-Alex et al., 2012)
	Na-Be	<100 µm	7	15-120	9.9	Present study
	Na-Be450	<100 µm	7	15-120	10.7	Present study
Ag	Na-Montmorillonite	-	4.1	10-110	3.7	(Chen et al., 2015)
	Clinoptilolite	-	4	10-150	33.23	(Akgül et al., 2006)
	Expanded perlite	-	2-8	5-50	8.46	(Ghassabzadeh et al., 2010)
	Calcareous soils	<2 mm	5.8	2-500	3.65	(Rahmatpour et al., 2017)
	Na-Be	<100 µm	7	15-120	6.6	Present study
	Na-Be450	<100 µm	7	15-120	7.1	Present study

3.7. Regeneration study

The regeneration and reuse of Na-Be and Na-Be450 adsorbents is an interesting operation from an environmental and economical point of view if an industrial application is targeted. The impact of regeneration cycles on efficiency removal is presented in Figure 9. The regeneration efficiency showed that nickel adsorption efficiency on Na-Be450 and Na-Be (B and C bars) was kept around 90%, and 70%, respectively, up to the fifth cycle of regeneration. For Ag, both Na-Be450 and Na-Be (D and E bars) removal efficiency dramatically decreased from the first cycle of regeneration until the fifth one. nickel retention through regeneration cycles show that Na-Be and Na-Be450 can be easily regenerated and still demonstrated a high efficiency, sustainable in time.

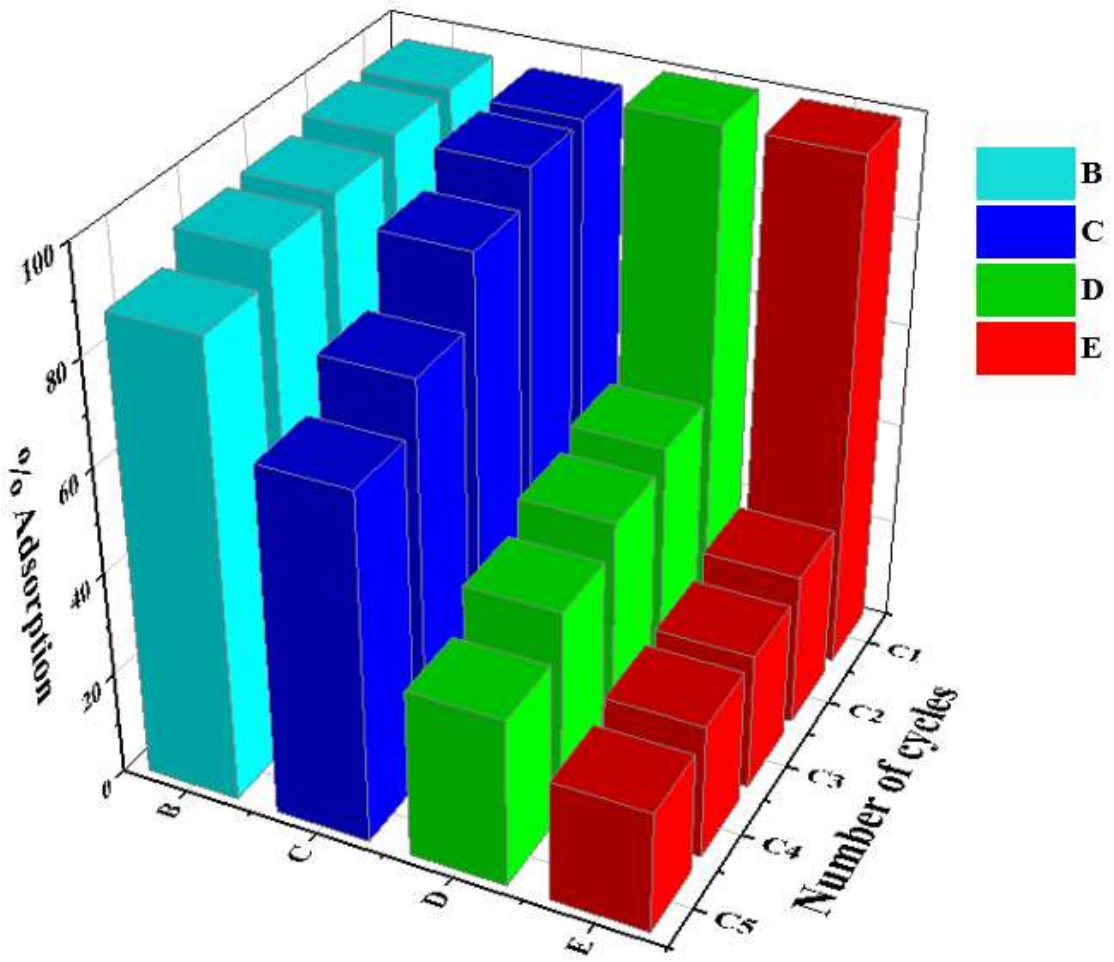

Fig.9. Ni retention through regeneration cycles onto Na-Be 450 (**B**) and Na-Be (**C**) as well as Ag retention through regeneration cycles onto Na-Be450 (**D**) and Na-Be (**E**).

4. Conclusion

In this paper, a Na_2CO_3-activated bentonite (Na-Be) and modified by combined chemical and thermal activation (Na-Be450). Both treatments of the bentonite led to improving the specific surface areas of the material and its adsorption capacity.

The sorption experiments carried out has shown that Na-Be and Na-Be450 materials demonstrated a noticeable retention ability towards nickel and silver, taken separately or as a binary-component system. The contact time was rapid, which turns these materials suitable for industrial depolluting systems. In single component system, the maximum nickel and silver retention capacity was obtained on Na-Be450, which fully follows the variation of specific surface with activation treatment. The adsorption isotherms were

better represented by the L-F Model suggesting that the monolayer adsorption of nickel and silver onto Na-Be and Na-Be450. The results in binary-component systems confirms the previous results in single-component systems. This study showed the positive effect of combined chemical and thermal activation on the enhancing adsorbent properties. The use of Na-Be and Na-Be450 were then successfully tested in industrial effluents: brassware effluent as well as river effluents, demonstrating the possible use of this worldwide materials in wastewaters treatment. Finally, the regeneration study revealed a net benefit for Na-Be450, which make it as low-cost effective adsorbent.

Acknowledgement

The authors wish to thank Mr. M. Akhazzane (USMBA, Morocco) for easing the access to some analytical apparatus and their help during the measurements, as well as the Academy of Finland.

References

Aithani, D., Jyethi, D.S., Siddiqui, Z., Yadav, A.K., Khillare, P.S., 2020. Source apportionment, pollution assessment, and ecological and human health risk assessment due to trace metals contaminated groundwater along urban river floodplain. Groundw. Sustain. Dev. 11, 100445. https://doi.org/10.1016/j.gsd.2020.100445

Akgül, M., Karabakan, A., Acar, O., Yürüm, Y., 2006. Removal of silver (I) from aqueous solutions with clinoptilolite. Microporous Mesoporous Mater. 94, 99–104. https://doi.org/10.1016/j.micromeso.2006.02.023

Akpomie, K.G., Dawodu, F.A., 2014. Efficient abstraction of nickel(II) and manganese(II) ions from solution onto an alkaline-modified montmorillonite. J. Taibah Univ. Sci. 8, 343–356. https://doi.org/10.1016/j.jtusci.2014.05.001

Aksu, Z., 2001. Equilibrium and kinetic modelling of cadmium(II) biosorption by C. Tulgaris in a batch system: effect of temperature. Sep. Purif. Technol. 21, 285–294. https://doi.org/10.1016/j.desal.2006.04.052

Alvarez-Ayuso and Garcia-Sanchez, 2003. Removal Of Heavy Metals From Waste Waters By Natural And Na-Exchanged Bentonites. Clays Clay Miner. 51, 475–480. https://doi.org/10.1346/CCMN.2003.0510501

Ansanay-Alex, S., Lomenech, C., Hurel, C., Marmier, N., 2012. Adsorption of nickel and arsenic from aqueous solution on natural sepiolite. Int. J. Nanotechnol. 9, 204–215. https://doi.org/10.1504/IJNT.2012.045327

Ayari, F., Srasra, E., Trabelsi-Ayadi, M., 2005. Characterization of bentonitic clays and their use as adsorbent. Desalination 185, 391–397. https://doi.org/10.1016/j.desal.2005.04.046

Bertagnolli, C., Kleinübing, S.J., Gurgel, M., 2011. Preparation and characterization of a Brazilian bentonite clay for removal of copper in porous beds. Appl. Clay Sci. 53, 73–79. https://doi.org/10.1016/j.clay.2011.05.002

Bhattacharyya, K.G., Gupta, S. Sen, 2008. Adsorption of a few heavy metals on natural and modified kaolinite and montmorillonite: A review. Adv. Colloid Interface Sci. 140, 114–131. https://doi.org/10.1016/j.cis.2007.12.008

Bódalo-Santoyo, A., Gómez-Carrasco, J.L., Gómez-Gómez, E., Máximo-Martín, F., Hidalgo-Montesinos, A.M., 2003. Application of reverse osmosis to reduce pollutants present in industrial wastewater. Desalination 155, 101–108. https://doi.org/10.1016/S0011-9164(03)00287-X

Carvalho, W.A., Vignado, C., Fontana, J., 2008. Ni (II) removal from aqueous effluents by silylated clays. Hazard. Mater. 153, 1240–1247. https://doi.org/10.1016/j.jhazmat.2007.09.083

Chen, C., Liu, H., Chen, T., Chen, D., Frost, R.L., 2015. An insight into the removal of Pb(II), Cu(II), Co(II), Cd(II), Zn(II), Ag(I), Hg(I), Cr(VI) by Na(I)-montmorillonite and Ca(II)-montmorillonite. Appl. Clay Sci. 118, 239–247. https://doi.org/10.1016/j.clay.2015.09.004

Da, A., Robens, E., 2004. Selective removal of the heavy metal ions from waters and industrial wastewaters by ion-exchange method. Chemosphere 56, 91–106. https://doi.org/10.1016/j.chemosphere.2004.03.006

Das, K.K., Das, S.N., Dhundasi, S.A., 2008. Nickel, its adverse health effects & oxidative stress. Indian J. Med. Res. 128, 412–425.

Dey, S., Podder, S., Roychowdhury, A., Das, D., Kr, C., 2018. Facile synthesis of hierarchical nickel (III) oxide nanostructure : A synergistic remediating action towards water contaminants. J. Environ. Manage. 211, 356–366. https://doi.org/10.1016/j.jenvman.2018.01.009

Dotto, G.L., Cunha, J.M., Calgaro, C.O., Tanabe, E.H., Bertuol, D.A., 2015. Surface modification of chitin using ultrasound-assisted and supercritical CO2 technologies for cobalt adsorption. J. Hazard. Mater. 295, 29–36. https://doi.org/10.1016/j.jhazmat.2015.04.009

El Miz, M., Akichoh, H., Berraaouan, D., Salhi, S., Tahani, A., 2017. Chemical and Physical Characterization of Moroccan Bentonite Taken from Nador (North of Morocco). Am. J. Chem. 2017, 105–112. https://doi.org/10.5923/j.chemistry.20170704.01

El Ouardi, Y., Branger, C., Laatikainen, K., Durrieu, G., Mounier, S., Lenoble, V., Ouardi, Y. El, Branger, C., Laatikainen, K., Durrieu, G., Mounier, S., 2020. Impact of thermal treatment on bentonite retention ability toward nickel and silver retention. Sep. Sci. Technol. 55, 1–11. https://doi.org/10.1080/01496395.2020.1839772

El Ouardi, Y., Branger, C., Toufik, H., Laatikainen, K., Ouammou, A., Lenoble, V., 2020. An insight of enhanced natural material (calcined diatomite) efficiency in nickel and silver

retention: application to natural effluents. Environ. Technol. Innov. 18, 100768. https://doi.org/https://doi.org/10.1016/j.eti.2020.100768

El Samrani, A.G., Lartiges, B.S., Villiéras, F., 2008. Chemical coagulation of combined sewer overflow: Heavy metal removal and treatment optimization. Water Res. 42, 951–960. https://doi.org/10.1016/j.watres.2007.09.009

Er-ramly, A., 2014. Physicochemical and Mineralogical Characterization of Moroccan Bentonite of Trebia and Its Use in Ceramic Technology. Am. J. Phys. Chem. 3, 96. https://doi.org/10.11648/j.ajpc.20140306.12

España, V.A.A., Sarkar, B., Biswas, B., Rusmin, R., Naidu, R., 2019. Environmental applications of thermally modified and acid activated clay minerals: Current status of the art. Environ. Technol. Innov. 13, 383–397. https://doi.org/10.1016/j.eti.2016.11.005

EU, 2008. Directive 2008/105/EC of the European Parliament and of the Council of 16 December 2008 on environmental quality standards in the field of water policy, amending and subsequently repealing Council Directives 82/176/EEC, 83/513/EEC, 84/156/EEC,84/491/EEC,. Off. J. Eur. Union L348/84-L348/97. https://doi.org/http://eur-lex.europa.eu/legal-content/EN/TXT/?uri=celex:32008L0105

EU, 1998. Council Directive 98/83/EC of 3 November 1998 on the quality of water intended for human consumption, Official Journal of the European Communities. https://doi.org/10.1017/cbo9780511610851.055

Fabrega, J., Luoma, S.N., Tyler, C.R., Galloway, T.S., Lead, J.R., 2011. Silver nanoparticles : Behaviour and effects in the aquatic environment. Environ. Int. 37, 517–531. https://doi.org/10.1016/j.envint.2010.10.012

Farmer, V.C., 1974. Infrared spectra of minerals. Mineral. Soc. Monogr. 4 539.

Freitas, E.D., Carmo, A.C.R., Neto, A.F.A., Vieira, M.G.A., 2017. Binary adsorption of silver and copper on Verde-lodo bentonite : Kinetic and equilibrium study. Appl. Clay Sci. 137, 69–76.

Freundlich, H., 1906. Über die Adsorption in Lösungen. Zeitschrift für Phys. Chemie 57, 385–470.

Fu, F., Wang, Q., 2011. Removal of heavy metal ions from wastewaters : A review. J. Environ. Manage. 92, 407–418. https://doi.org/10.1016/j.jenvman.2010.11.011

G. Socrates, 2001. Infrared and Raman Characteristic Group Frequencies. Tables and Charts, John Wiley and Sons. Chichester.

Ghassabzadeh, H., Mohadespour, A., Torab-mostaedi, M., Zaheri, P., Ghannadi, M., Taheri, H., 2010. Adsorption of Ag , Cu and Hg from aqueous solutions using expanded perlite. J. Hazard. Mater. 177, 950–955. https://doi.org/10.1016/j.jhazmat.2010.01.010

Guerra, D.J.L., Mello, I., Resende, R., Silva, R., 2013. Application as absorbents of natural and functionalized Brazilian bentonite in Pb2+ adsorption: Equilibrium, kinetic, pH, and thermodynamic effects. Water Resour. Ind. 4, 32–50. https://doi.org/10.1016/j.wri.2013.11.001

Guimarães, D., Leão, V.A., 2014. Batch and fixed-bed assessment of sulphate removal by the weak base ion exchange resin Amberlyst A21. J. Hazard. Mater. 280, 209–215. https://doi.org/10.1016/j.jhazmat.2014.07.071

Gulbranson, S.H., Hud, J.A., Hansen, R.C., 2000. Argyria following the use of dietary supplements containing colloidal silver protein. Cutis 66, 1–3.

Ho, Y.S., 2006. Review of second-order models for adsorption systems. J. Hazard. Mater. 136, 681–689. https://doi.org/10.1016/j.jhazmat.2005.12.043

Ignasi Puigdomenech, 2015. Hydra/Medusa Chemical Equilibrium Database and Plotting Software (2015) [WWW Document]. URL https://www.kth.se/che/medusa

Ijagbemi, C.O., Baek, M.H., Kim, D.S., 2010. Adsorptive performance of un-calcined sodium exchanged and acid modified montmorillonite for Ni2+ removal: Equilibrium, kinetics, thermodynamics and regeneration studies. J. Hazard. Mater. 174, 746–755. https://doi.org/10.1016/j.jhazmat.2009.09.115

Islam, M.S., Tanaka, M., 2004. Impacts of pollution on coastal and marine ecosystems including coastal and marine fisheries and approach for management: A review and synthesis. Mar. Pollut. Bull. 48, 624–649. https://doi.org/10.1016/j.marpolbul.2003.12.004

Karapinar, N., Donat, R., 2009. Adsorption behaviour of Cu2+ and Cd2+ onto natural bentonite. Desalination 249, 123–129. https://doi.org/10.1016/j.desal.2008.12.046

Katsou, E., Malamis, S., Haralambous, K.J., Loizidou, M., 2010. Use of ultrafiltration membranes and aluminosilicate minerals for nickel removal from industrial wastewater. J. Memb. Sci. 360, 234–249. https://doi.org/10.1016/j.memsci.2010.05.020

Kumar, P.S., Ramalingam, S., Kirupha, S.D., Murugesan, A., Vidhyadevi, T., Sivanesan, S., 2011. Adsorption behavior of nickel(II) onto cashew nut shell: Equilibrium, thermodynamics, kinetics, mechanism and process design. Chem. Eng. J. 167, 122–131. https://doi.org/10.1016/j.cej.2010.12.010

Lagergren, S., 1898. About the theory of so-called adsorption of soluble substances. Sven Vetenskapsakad Handl. 24, 1–39.

Langmuir, I., 1918. The adsorption of gases on plane surfaces of glass, mica and platinum. J. Am. Chem. Soc. 345, 1361–1403.

Lin, Y.C., Hsu, S.C., Chou, C.C.K., Zhang, R., Wu, Y., Kao, S.J., Luo, L., Huang, C.H., Lin, S.H., Huang, Y.T., 2016. Wintertime haze deterioration in Beijing by industrial pollution deduced from trace metal fingerprints and enhanced health risk by heavy metals. Environ. Pollut. 208, 284–293. https://doi.org/10.1016/j.envpol.2015.07.044

Liu, Y., Liu, C., Rong, Q., Zhang, Z., 2003. Characteristics of the silver-doped TiO 2 nanoparticles. Appl. Surf. Sci. 220, 7–11. https://doi.org/10.1016/S0169-4332(03)00836-5

Maillard, J.Y., Hartemann, P., 2013. Silver as an antimicrobial: facts and gaps in knowledge. Crit. Rev. Microbiol. 39, 373–383. https://doi.org/10.3109/1040841X.2012.713323

Mckay, Y.S.H. and G., 1998. Kinetic models for the sorption of dye From aqueous solution by wood. Process Saf. Environ. Prot. 76, 183–191.

Mohammed-Azizi, F., Dib, S., Boufatit, M., 2013. Removal of heavy metals from aqueous solutions by Algerian bentonite. Desalin. Water Treat. 51, 4447–4458. https://doi.org/10.1080/19443994.2013.770241

Mohan, D., Singh, K.P., 2002. Single- and multi-component adsorption of cadmium and zinc using activated carbon derived from bagasse F an agricultural waste $. Water Res. 36, 2304–

2318.

Motsi, T., Rowson, N.A., Simmons, M.J.H., 2009. Adsorption of heavy metals from acid mine drainage by natural zeolite. Int. J. Miner. Process. 92, 42–48. https://doi.org/10.1016/j.minpro.2009.02.005

Mousavi, M.P.S., Gunsolus, I.L., Pérez De Jesús, C.E., Lancaster, M., Hussein, K., Haynes, C.L., Bühlmann, P., 2015. Dynamic silver speciation as studied with fluorous-phase ion-selective electrodes: Effect of natural organic matter on the toxicity and speciation of silver. Sci. Total Environ. 537, 453–461. https://doi.org/10.1016/j.scitotenv.2015.07.151

Mulk, S., Korai, A.L., Azizullah, A., Khattak, M.N.K., 2016. Decreased fish diversity found near marble industry effluents in River Barandu, Pakistan. Ecotoxicology 25, 132–140. https://doi.org/10.1007/s10646-015-1575-9

Nagajyoti, P.., Lee, K.., Sreekanth, T.., 2010. Heavy metals, occurrence and toxicity for plants: a review. Environ. Chem. Lett. 8, 199–216.

Özcan, A., Ömeroğlu, Ç., Erdoğan, Y., Özcan, A.S., 2007. Modification of bentonite with a cationic surfactant: An adsorption study of textile dye Reactive Blue 19. J. Hazard. Mater. 140, 173–179. https://doi.org/10.1016/j.jhazmat.2006.06.138

Piccin, J.S., Cadaval, T.R.S.A., De Pinto, L.A.A., Dotto, G.L., 2017. Adsorption isotherms in liquid phase: Experimental, modeling, and interpretations, Adsorption Processes for Water Treatment and Purification. https://doi.org/10.1007/978-3-319-58136-1_2

Qing, X., Yutong, Z., Shenggao, L., 2015. Assessment of heavy metal pollution and human health risk in urban soils of steel industrial city (Anshan), Liaoning, Northeast China. Ecotoxicol. Environ. Saf. 120, 377–385. https://doi.org/10.1016/j.ecoenv.2015.06.019

Rahmatpour, S., Shirvani, M., Mosaddeghi, M.R., 2017. Retention of silver nano-particles and silver ions in calcareous soils : Influence of soil properties. J. Environ. Manage. 193, 136–145. https://doi.org/10.1016/j.jenvman.2017.01.062

Rivera, I., Roca, A., Cruells, M., Patiño, F., Salinas, E., 2007. Study of silver precipitation in thiosulfate solutions using sodium dithionite. Application to an industrial effluent. Hydrometallurgy 89, 89–98. https://doi.org/10.1016/j.hydromet.2007.06.001

Etris, S.F., 2010. Silver and silver alloys. Kirk-Othmer Encycl. Chem. Technol. https://doi.org/https://doi.org/10.1002/0471238961.1909122205201809.a01.pub3

Shichi, T., Takagi, K., 2000. Clay minerals as photochemical reaction fields. J. Photochem. Photobiol. C Photochem. Rev. 1, 113–130. https://doi.org/10.1016/S1389-5567(00)00008-3

Stafford, K., Sing, W., Rouquerol, J., 1985. Reporting physisorption data for gas/solid systems with Special Reference to the Determination of Surface Area and Porosity. Pure Applied.Chemistry 57, 603–619.

Thommes, M., Kaneko, K., Neimark, A. V, Olivier, J.P., Rodriguez-reinoso, F., Rouquerol, J., Sing, K.S.W., 2015. Physisorption of gases , with special reference to the evaluation of surface area and pore size distribution (IUPAC Technical Report). Pure Appl. Chem. https://doi.org/10.1515/pac-2014-1117

Uddin, M.K., 2017. A review on the adsorption of heavy metals by clay minerals , with special focus on the past decade. Chem. Eng. J. 308, 438–462.

https://doi.org/10.1016/j.cej.2016.09.029

Vieira, M.G.A., Neto, A.F.A., Gimenes, M.L., Silva, M.G.C., 2010a. Removal of nickel on Bofe bentonite calcined clay in porous bed. J. Hazard. Mater. 176, 109–118. https://doi.org/10.1016/j.jhazmat.2009.10.128

Vieira, M.G.A., Neto, A.F.A., Gimenes, M.L., Silva, M.G.C., 2010b. Sorption kinetics and equilibrium for the removal of nickel ions from aqueous phase on calcined Bofe bentonite clay. J. Hazard. Mater. 177, 362–371. https://doi.org/10.1016/j.jhazmat.2009.12.040

Vorkamp, K., Sanderson, H., 2016. European Environmental Quality Standards (EQS) Variability Study: Analysis of the variability between national EQS values across Europe for selected Water Framework Directive River Basin-Specific Pollutants, Aarhus University, DCE – Danish Centre for Environment and Energy.

Xu, W., Johnston, C.T., Parker, P., Agnew, S.E., 2000. Infrared study of water sorption on Na- , Li- , Ca- , and Mg-exchanged (SWy- 1 and SAz- 1) Montmorillonite. Clays' Clay Miner. 120–131.

Yang, Q., Li, Z., Lu, X., Duan, Q., Huang, L., Bi, J., 2018. A review of soil heavy metal pollution from industrial and agricultural regions in China: Pollution and risk assessment. Sci. Total Environ. 642, 690–700. https://doi.org/10.1016/j.scitotenv.2018.06.068

Yavuz, Ö., Altunkaynak, Y., Güzel, F., 2003. Removal of copper, nickel, cobalt and manganese from aqueous solution by kaolinite. Water Res. 37, 948–952. https://doi.org/10.1016/S0043-1354(02)00409-8

Yildiz, N., Sarikaya, Y., Çalimli, A., 1999. The effect of the electrolyte concentration and pH on the rheological properties of the original and the Na2CO3-activated Kutahya bentonite. Appl. Clay Sci. 14, 319–327. https://doi.org/10.1016/S0169-1317(99)00006-X

Zaini, M.A.A., Amano, Y., Machida, M., 2010. Adsorption of heavy metals onto activated carbons derived from polyacrylonitrile fiber. J. Hazard. Mater. 180, 552–560. https://doi.org/10.1016/j.jhazmat.2010.04.069

Zhi-rong, L., Shao-qi, Z., 2009. Adsorption of copper and nickel on Na-bentonite. Process Saf. Environ. Prot. 88, 62–66. https://doi.org/10.1016/j.psep.2009.09.001

Zhu, H., Xiao, X., Guo, Z., Han, X., Liang, Y., Zhang, Y., Zhou, C., 2018. Adsorption of vanadium (V) on natural kaolinite and montmorillonite: Characteristics and mechanism. Appl. Clay Sci. 161, 310–316. https://doi.org/10.1016/j.clay.2018.04.035

Zou, W., Han, R., Chen, Z., Jinghua, Z., Shi, J., 2006. Kinetic study of adsorption of Cu(II) and Pb(II) from aqueous solutions using manganese oxide coated zeolite in batch mode. Colloids Surfaces A Physicochem. Eng. Asp. 279, 238–246. https://doi.org/10.1016/j.colsurfa.2006.01.008